journal homepage: http://www.jsoftcivil.com/

Structural Response of Reinforced Self-Compacting Concrete Deep Beam using Finite Element Method

M. A. Akinpelu[1*] and A. A. Adedeji[2]

1. Lecturer, Department of Civil Engineering, College of Engineering and Technology, Kwara State University, Malete, Kwara State, Nigeria
2. Professor, Department of Civil Engineering, Faculty of Engineering and Technology, Ilorin, Nigeria

Corresponding author: *mutiu.akinpelu@kwasu.edu.ng*

ARTICLE INFO

Article history:
Received: 01 August 2017
Accepted: 14 September 2017

Keywords:
Self-compacting concrete,
Deep beam,
Concrete damage plasticity,
FEM.

ABSTRACT

Analysis of reinforced concrete deep beam is based on simplified approximate method due to the complexity of the exact analysis. The complexity is due to a number of parameters affecting its response. To evaluate some of this parameters, finite element study of the structural behaviour of reinforced self-compacting concrete deep beam was carried out using Abaqus finite element modeling tool. The model was validated against experimental data from literature. The parametric effects of varied concrete compressive strength, vertical web reinforcement ratio and horizontal web reinforcement ratio on the beam were tested on eight (8) different specimens under four point loads. The results of the validation work showed good agreement with the experimental studies. The parametric study revealed that the concrete compressive strength most significantly influenced the specimens' response with the average of 41.1% and 49 % increment in the diagonal cracking and ultimate load respectively due to doubling of concrete compressive strength. Although increase in horizontal web reinforcement ratio from 0.31 % to 0.63 % lead to average of 6.24 % increment on the diagonal cracking load, it does not influence the ultimate strength and the load deflection response of the beams. Similar variation in vertical web reinforcement ratio lead to average of 2.4 % and 15 % increment in cracking and ultimate load respectively with no appreciable effect on the load deflection response.

1. Introduction

Deep beams are members that are loaded on one face and supported on the other face such that strut-like compression element can develop between the loads and the supports provided that the

clear span does not exceed four times the overall depth or concentrated load exists within a distance of two times the overall depth of the beam from the face of the support [1]. Euro Code [2] on the hand does not account for the difference in the loading distribution. It defines a deep beam as a member whose span is less to or equal to 3 times the overall section depth. Due to the small span to depth ratio, deep beam supports heavy loads with little or no deflection, hence it is utilized in many structural applications requiring heavy load transfer such as bridges, diaphragms, water tanks, foundations, bunkers, girders used in multi-story buildings to provide column offsets and floor slabs under horizontal loads [3]. Typically, deep beams have narrow width and contains congested arrangement of reinforcements making it difficult for convectional vibrated concrete (VC) to flow easily through its web and adequately fill the bottom part. This often results in many problems in concrete such as voids, segregation, weak bond with reinforcement bars and holes in its surface [4]. It is on this ground that some studies have recommended the use of self-compacting concrete (SCC) for casting structural members such as deep beam [4].

SCC is an innovative concrete that is able to flow under its own weight, completely fill the formwork and achieve full compaction, even in the presence of congested reinforcement without segregation [5]. It has gained preference over vibrated concrete due to a number of factors, including: faster construction, reduction in site manpower, better surface finishes, easier placing, improved durability, greater freedom in the design of thinner concrete sections, reduced noise levels, absence of vibration and safer working environment [6]. Comprehensive studies have been presented in literatures on the compositions and mechanical properties of SCC [5, 7].

The difference in some of the mechanical properties and mix compositions of the vibrated concrete (VC) and the self-compacting concrete (SCC) demands investigation of the structural behaviour of members constructed using this type of concrete. Of major concern to researchers is the shear strength of deep beams. It is argued that the aggregate interlock mechanism, which is partly responsible for shear strength of the structure, is likely to be weaker in SCC since it contains fewer and smaller sizes of coarse aggregate compare to vibrated concrete. Choi et al. [8]experimented four deep beam specimens (two made with SCC and two with VC) to evaluate the influence of the concrete types on the shear strength of deep beams. The study reported that the SCC specimen having normal shear reinforcement distribution showed slightly higher

performance than the corresponding VC specimen, while the SCC specimen having congested shear reinforcement condition showed a similar load carrying capacity to the corresponding VC specimen. The work of Itterbeeck et al. [9] on shear capacity of SCC beams also reported improved shear strength over VC. On the contrary, Biolzi *et al.* (2014), as cited in [10], concluded that the ultimate shear strength of SCC beams is lower than that of VC beams.

Structural design of deep beams is another area of great concern. The complex stress distribution in deep beam cannot be resolved with the technical bending theory since the assumption of linear strain distribution cease to be valid and hence, the section of the beam belong to Disturbed-region (D-region) [11]. Previously, D-region has been designed based on rule of thumb or purely experimental model [12]. The most recent approach to the design of D-region uses the strut and tie model (STM). It is a simplified method in which the continuous reinforced concrete domain is transformed to an equivalent truss as shown in Figure 1. The compression and tension zones are converted into equivalent struts and ties connected at the nodes to form a truss which can be easily resolved using basic mechanics [1]

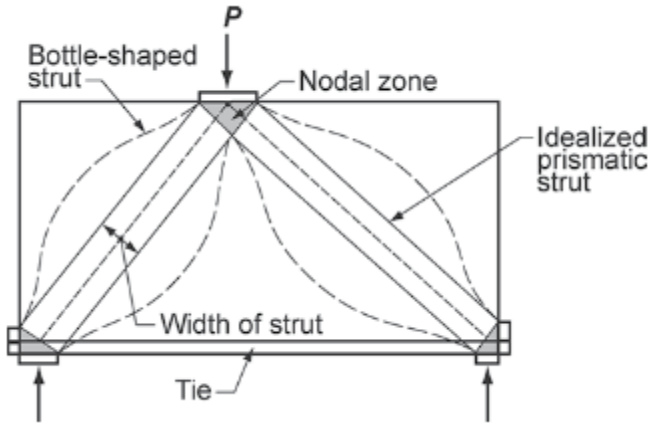

Fig. 1. Strut and tie model of deep beam [1]

Despite the simplicity of the STM approach, there is no clear guide to define the geometry of the strut and tie model [13]. The major complexity is about transforming the continuous structural domain to optimal strut and tie model (STM). As reported by Liang et al. [13], Ritter (1899) found that a reinforced concrete beam after cracking due to diagonal tensile stresses could be modelled as a parallel chord truss with compressive diagonals inclined at 45^{o} with respect to the longitudinal axis of the beam. Schlaich et al. [12] also recommended elastic stress method and load path method.

The reported techniques for developing STM involve trial and error iterative process which depend on the intuition and experience of the designer. Previous knowledge of stress distribution within the design domain is also necessary so as to reduce the number of iterative processes required to achieve adequate truss model. These lead to analysis result that are not unique but depend on the truss configurations. Therefore, alternative deign procedure is required to achieve uniform and efficient save design of deep beam. To achieve this, proper characterization of various factors influencing the strength properties of deep beam is worthy of evaluation.

In the past, experimental procedure is mostly preferred as it provides real life structural behavior that can be guaranteed of high accuracy. However, the need to execute the experimental study in line with standard specifications often make the procedure expensive and time consuming. Besides, there are some other real life situations that do not demand experimental work. In practice, there are many instances that performance assessment of structures incorporating deep beam is required due to changes in design codes, specifications, occurrence of damage or degradation under service condition. Another case is when a constructed structure faces new conditions and needs to be retrofitted or repaired. Hence, the recent trends favoured the use of numerical methods to evaluate the structural behaviour of members. One of the most widely utilized approach is the finite element methods (FEM).

Ever since the introduction of FEM in Civil Engineering, it has been an effective tool for modeling and simulation of both linear and nonlinear behaviour of reinforced concrete structures. Recent advancement in computational mechanics has also lead to the development of numerous material models that are compatible with finite element analysis method. In the present study, finite element model of reinforced self-compacting concrete deep beam was developed using Abaqus finite element modelling tool. The aim of the study was to investigate the structural response of Reinforced Self-Compacting Concrete (RSCC) deep beam. The specific objectives of the study were (i) to validate the capability of the finite element (FE) model to capture the behaviour of RSCC deep beam up till failure and (ii) to evaluate the parametric effect of some of the beam parameters on the structural behaviour of the beam. The parameters studied are concrete compressive strength, vertical web reinforcement and horizontal web reinforcement of the beams.

2. Research Program

This study was conducted in two phases. The first phase of the work involved the validation of the FE model results against the experimental values from literature. The second phase focused on the parametric study to evaluate the influence of various design parameter on the load deflection response, failure load, as well as failure mode of deep beam.

2.1. Model Validation

In order to demonstrate the capability of the FE model to simulate the response of reinforced self-compacting concrete (RSCC) deep beam under load up till failure, data on two (2) RSCC deep beam specimens previously tested by Choi et al. [8] were obtained from literature. The beams have the similar geometrical properties but different shear reinforcement distributions; were tested to failure under 4-point loadings. The goal of the tests was to study the behaviour and performance RSCC deep beam. The detailed configuration of the experimental set-up is shown in Figure 2 while the reported results of the mechanical property tests on reinforcing steels and concrete were presented in Table 1 and Table 2 respectively.

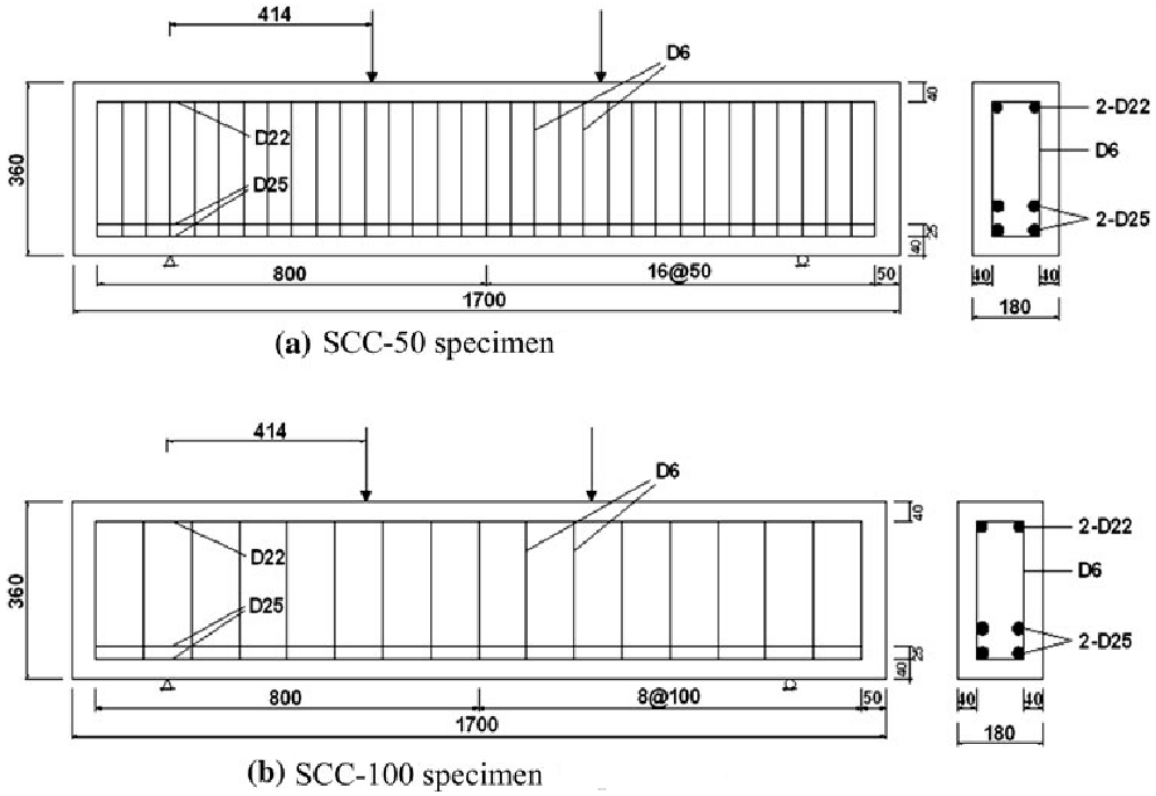

Fig. 2. Details and Dimensions of deep of beams (All dimensions in mm) [8]

Table 1. Mechanical properties for the reinforcement steel [8]

Bar Diameter (mm)	Yield Stress (N/mm^2)	Ultimate Stress (N/mm^2)	Elongation (%)
25	334	512	33
22	347	542	25
6	447	743	21

Table 2. Mechanical properties for the self-compacting concrete [8]

Mix Code	Compressive strength, f_c (N/mm^2)	Tensile Strength, f_t (N/mm^2)	Modulus of Elasticity, E (N/mm^2)
HSCC	52.1	4.2*	37677.76*

The tensile strength, f_t and the modulus of elasticity, E for the concrete were not reported in the study. The parameters were however obtained using the mathematical models in equations (1) and (2) respectively as given in [2].

$$f_t = 0.3 * {f_c}^{2/3} \quad (1)$$

$$E = 22[(f_c + 8)/10]^{0.3} * 10^3 \quad (2)$$

2.2. Parametric Study

The primary goal of numerical simulation is to create platform for parametric studies. In this work, the validated FE model was employed to evaluate the influence of various beam design parameters on the behavior of RSCC deep beam. Eight deep beams of the same geometrical dimension but different concrete compressive strengths, vertical and horizontal web reinforcement distributions as shown in Table 3 were modeled and analyzed. The beams' cross section dimension is 180 by 360 mm and the effective length is 1300 mm. The reported material properties in Table 1 and 2 were adopted for the parametric studies.

Table 3. Parameters of the modelled deep beam specimens

Beam Code	Total Length (mm)	Cross Section Dimension (mm)	a/d	Tension Reinforcement	Compression Reinforcement	Vertical Shear Reinforcement	Horizontal shear Reinforcement	Concrete Compressive strength (N/mm^2)
B1	1700	180 x 360	1.4	2ϕ25 + 2ϕ25	2ϕ22	ϕ6 / 100	ϕ6 / 100	52.10
B2	1700	180 x 360	1.4	2ϕ25 + 2ϕ25	2ϕ22	ϕ6 / 50	ϕ6 / 100	52.10
B3	1700	180 x 360	1.4	2ϕ25 + 2ϕ25	2ϕ22	ϕ6 / 100	ϕ6 / 100	26.05
B4	1700	180 x 360	1.4	2ϕ25 + 2ϕ25	2ϕ22	ϕ6 / 50	ϕ6 / 100	26.05
B5	1700	180 x 360	1.4	2ϕ25 + 2ϕ25	2ϕ22	ϕ6 / 100	ϕ6 / 50	52.10
B6	1700	180 x 360	1.4	2ϕ25 + 2ϕ25	2ϕ22	ϕ6 / 50	ϕ6 /50	52.10
B7	1700	180 x 360	1.4	2ϕ25 + 2ϕ25	2ϕ22	ϕ6 / 100	ϕ6 / 50	26.05
B8	1700	180 x 360	1.4	2ϕ25 + 2ϕ25	2ϕ22	ϕ6 / 50	ϕ6 / 50	26.05

3. Finite Element Study

The general purpose FE software, Abaqus [14] was used to develop FE models to mimic the structural response of the studied deep beams. The results of the simulation were compared to experimental results in term of load deflection responses, diagonal cracking and ultimate loads as well as failure patterns of the beams.

3.1 Concrete Constitutive Model

Abaqus software offers three different constitutive models to simulate the nonlinear response of concrete namely (1) Smeared crack model; (2) Discrete crack model; and (3) Damage plasticity model [14, 15]. The concrete damage plasticity model (CDPM) is the most preferred for this work due to the excellent performance recorded in similar studies [16, 17]. The CDPM as implemented in Abaqus software is based on the models proposed by Lubliner et al. (1989) and Lee and Fenves (1998) as cited in [15]. The model combines isotropic damaged elasticity model with isotropic tensile and compressive plasticity to represent the inelastic behaviour of concrete. It assumes that the main two failure mechanisms are tensile cracking and compressive crushing of the concrete material. The evolution of the yielding (or failure) is controlled by tensile and compressive equivalent plastic strains under tension and compression loading respectively. Figure 3 illustrates the uniaxial tensile and compressive behaviour of concrete as used in the CDPM. As depicted in the figure, the elastic stiffness of the material in the unloaded state is

damaged or degraded. The evolution of damage in tension and compression is controlled by the introduction of tensile and compressive damage variables, d_t and d_c which takes on values between 0 and 1 for initially undamaged material and completely damaged material respectively. Further explanation on the CDPM model can be found in [14, 15].

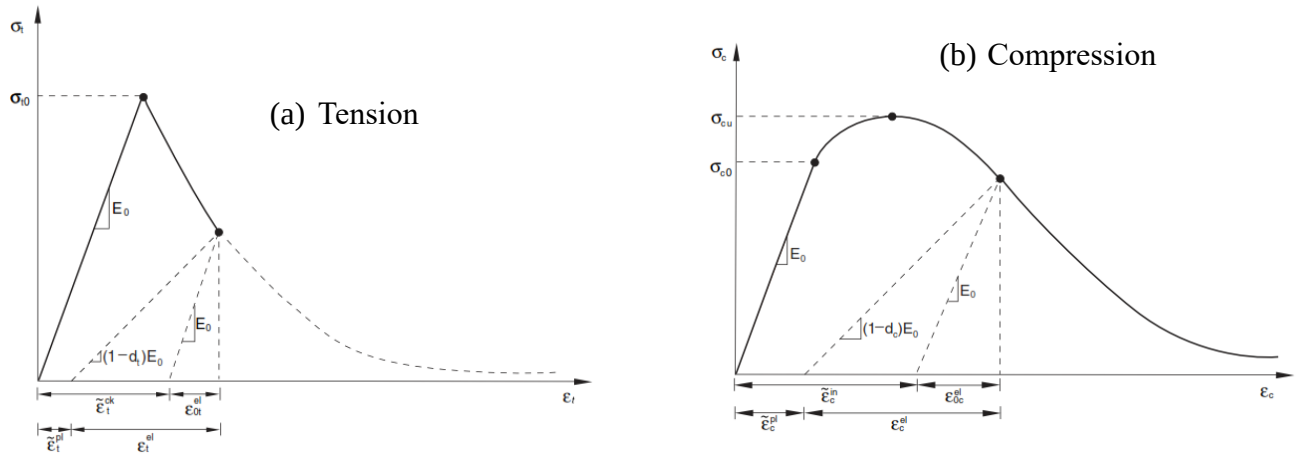

Fig. 3. Post failure stress-displacement curve [14]

3.1.1. Stress-Strain Relationship for Concrete in Compression

The stress-strain data for concrete in compression and tension is crucial for analysis utilising CDPM. However, this was not reported as part of the experimental results, only the ultimate compressive strength of the concrete at 28 days was recorded as given in Table 2. The curves were created using mathematical models found in literature. The compressive stress behaviour of concrete was generated using Eurocode 2 [2] model for non-linear structural analysis of concrete as shown in Figure 4.

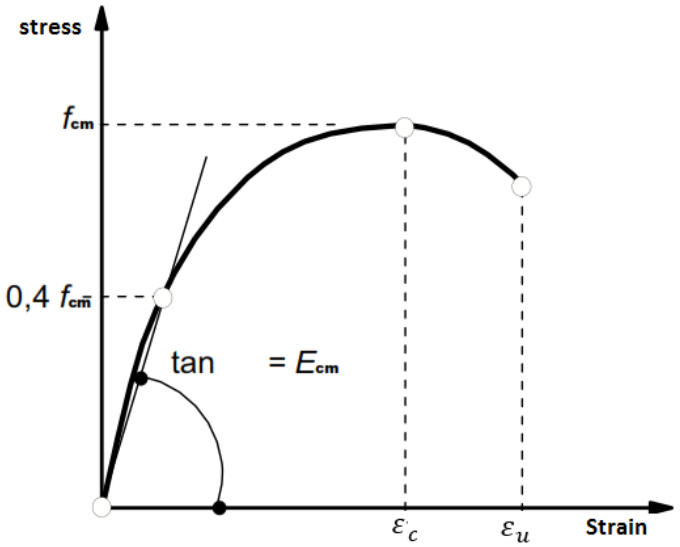

Fig. 4. Stress-strain model for concrete in compression [2]

The relationship between the compressive stress and shortening strain for short term uniaxial loading is as expressed in Equation (3).

$$\frac{\sigma_c}{f_{cm}} = \frac{k\eta - \eta^2}{1+(k-2)\eta} \tag{3}$$

The parameter in Equation (3) are epressed as follows:

$$\eta = \frac{\varepsilon_i}{\varepsilon_c} \tag{4}$$

$$\varepsilon_c = (0.7 {f_{cm}}^{0.31})/100 < 2.8 \tag{5}$$

$$\varepsilon_u = 0.0035 \quad (f_c < 50\, N/mm^2) \tag{6}$$

$$\varepsilon_u = (2.8 + 27[(98 - f_{cm})/100]^{\,4}/100 \qquad (f \geq 50\, N/mm^2) \tag{7}$$

$$k = 1.1E\ x\ (\varepsilon_u/f_{cm}) \tag{8}$$

$$f_{cm} = \mathrm{f_c} + 8\ (N/mm^2) \tag{9}$$

Where:

$\mathrm{f_c}$ is the characteristic cylindrical compressive strenght of concrete at 28 days

ε_c is the strain at peak stress

ε_u is the ultimate strain

3.1.2. Tensile stress Behaviour of Concrete

The nonlinear behaviour of concrete in tension is characterized by a stress-crack displacement response instead of a stress-strain relationship due to its brittle behaviour. This approach is preferred due to mesh sensitivity problem associated with stress-strain model for concrete in tension when there is no reinforcement in the significant region of the model [14]. The stress-crack displacement relationship can be model as linear, bilinear or exponential tension softening response as shown in Figure 5. For this study, the exponential stiffening curve according to Cornelissen et al., 1986, as cite in [18], was adopted.

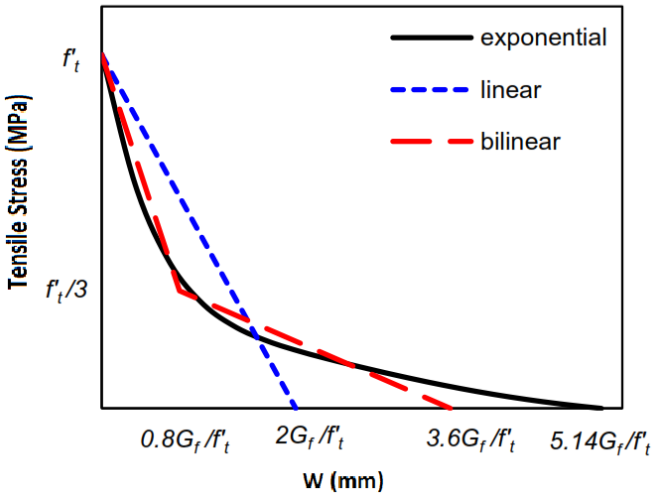

Fig. 5. Stress-crack width for concrete in tension [18]

The model governing equation is as stated in Equations (10) and (11).

$$\sigma/f_t = \left(1 + \left(\frac{c_1 w}{w_c}\right)^3\right) e^{-\frac{c_2 w}{w_c}} - (w/w_c)(1 + c_1^3)e^{-c_2} \quad (10)$$

$$w_c = 5.14\frac{G_f}{f_t'} \quad (11)$$

C1 and C2 are materials constants given as 3 and 6.93 for normal concrete, Wc is the critical crack opening width.

G_f is the fracture energy per unit area required to create, propagate and fully break a Mode 1 crack in concrete as given in Equation (12).

$$G_f = G_{fo}(f_{cm}/10)^{0.7} \quad (12)$$

G_{fo} is a coefficient which depends on the maximum size of aggregate. The coefficient can be obtained from [19]. The value used in this study is 0.08 J/m^2.

3.1.3. Other CDPM Parameters

(a) Dilation Angle, ψ accounts for the increase in plastic volume in concrete beyond the critical stress value. Different values of dilation angle for concrete are found in literature. Lubliner et al. (1989) as reported in [15] gives ψ as 30 for concrete. However, recent studies have successfully used higher values of ψ. For instance, Sumer and Aktas [20] used 37˚ while Demir et al. [21] adopted 56 ˚. Therefore, the appropriate value of ψ for this study was determined through sensitivity analysis. The values considered are 36˚, 46˚ and 56˚.

(b) Viscosity Parameter, μ is required for viscoplastic regularisation of the model. The value used for the study is 0.0001. The value is sufficiently small to enhance the rate of convergence without compromising the model results [22].

(c) Flow Potential Eccentricity, ϵ defines the rate at which the surface approaches its asymptote (the flow potential tends to a straight line as the eccentricity tends to zero). The parameter is calculated as the ratio of uniaxial tensile strength to uniaxial compressive strength. [23]

(d) The ratio of initial equibiaxial compressive yield stress to initial uniaxial compressive yield stress, $\frac{\sigma_{b0}}{\sigma_{c0}}$ was taken as 1.16 [15] . The ratio determines the point at which the material fails under biaxial compression

(e) K Parameter is the ratio of the second stress invariant on the tensile meridian to that on the compressive meridian at initial yield for any given value of the pressure invariant such that the maximum principal stress is negative. The default value of 0.667 was adopted [15].

3.2. Steel Reinforcement Constitutive Model

The steel material is assumed to be linearly elastic. The elastic modulus of 210 N/mm^2 and poison ratio of 0.3 were adopted for the material. The two elastic constants define the elastic isotropic properties the steel material. The experimental value of yield strengths presented in Table 1 with zero (0) plastic strain were used to defined the plasticity property of the material. These values defined the steel materials that were applied to the truss elements that modelled the steel reinforcements in the FE model.

3.3. Finite Element Model

All the studied beam specimens were model in Abaqus. The concrete was modelled with an 8-node linear solid element with reduced integration to prevent shear locking effect associated with fully integrated solid elements as noted in [14]. The reinforcement steel was modelled with 2-node 3D truss element since it supports only axial loads. The bonding of reinforcement with the concrete was ensured with an embedded constraint with the concrete as the host region. The mesh sizes considered for the study are 25 mm, 50 mm and 75 mm in all directions. This was done to observe the influence of mesh density on the results of the model. For the boundary conditions, the nodes at the supports were restrained against vertical displacement while the external nodes along the symmetry planes were restrained along the longitudinal and transverse directions respectively to allow for Poisson's effect. All the beams were loaded to failure by displacement control in the vertical direction from the datum point located above the beam and connected to the beam loading surface using equation constraint. Figure 6 shows a typical FE model for the beam section while Figure 7 shows the reinforcement model as embedded in the FE model.

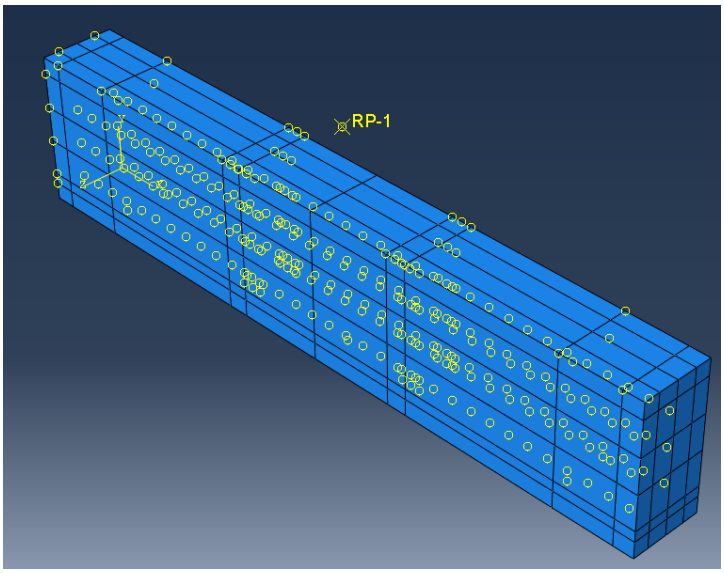

Fig. 6. Typical FE model of the deep beam specimens (Specimen B2)

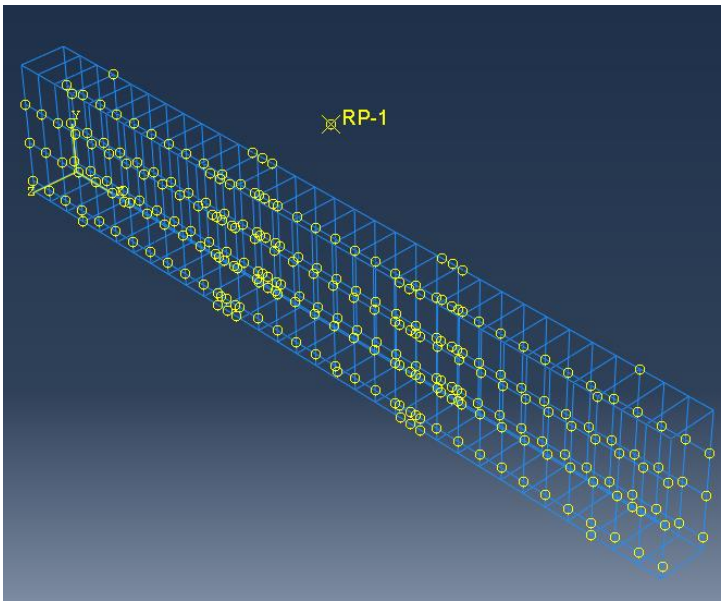

Fig. 7. Typical FE model of the reinforcement for the beam specimens (Specimen B2)

4. Results and Discussion

4.1. Model Sensitivity Analysis

4.1.1. Dilation Angle Sensitivity Analysis

Different values of dilation angle were reported for concrete in literature hence, the need to calibrate the parameter to select the most appropriate for the studied beam specimens. Figure 8 shows the results of the sensitivity tests. From the figure, the value of dilation angle that best modelled the experimental test is 56˚ and therefore used throughout the study. Table 4 gives the summary of other CDPM parameters finally adopted in the study.

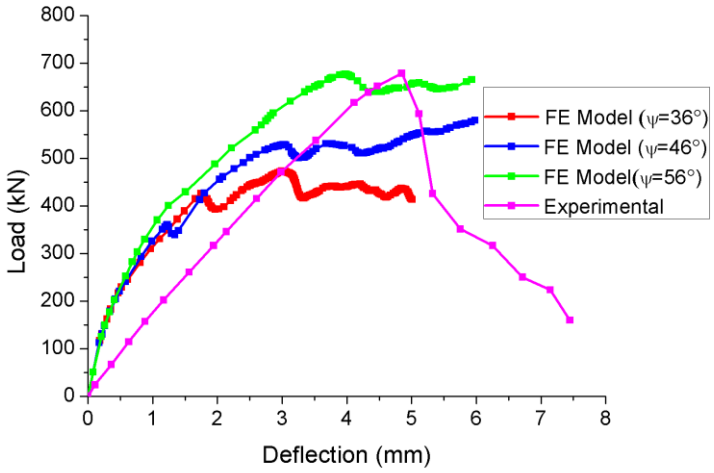

Figure 8: Dilation angle sensitivity test

Table 4: CDPM Model Parameters

Dilation Angle, ψ	56°
Viscosity, μ	0.0001
Eccentricity	0.1
Stress ratio	1.16
K	0.667

4.1.2. Mesh Sensitivity Analysis

Generally, FE models are sensitive to mesh density. Figure 9 shows the effect of mesh density on the load deflection response of the modelled beam specimen. The model with finer meshes captures the experimental result better than the model with coarse mesh although at higher computational time. The best convergence result is obtained with mesh size of 25 mm. This mesh size was used for the parametric study.

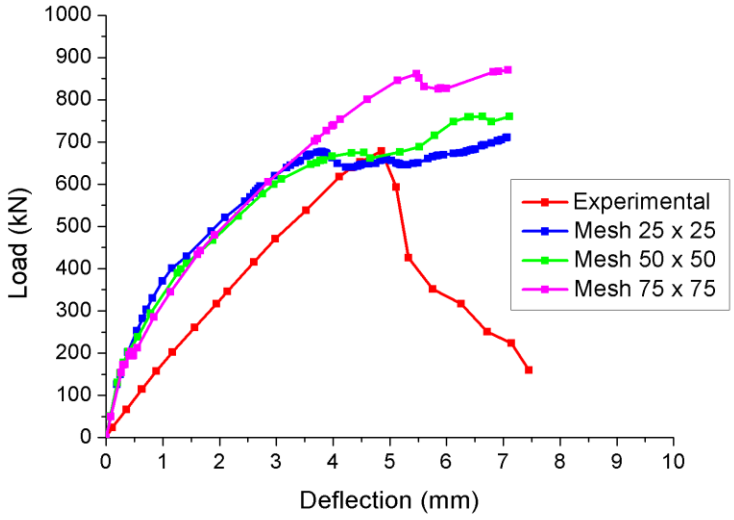

Fig. 9. Mesh sensitivity test

4.2. Model Validation

4.2.1. Load Deflection Response

The comparison of load deflection response of the FE model and the experimental results of the beam specimens are illustrated in Figure 10. From the figure, it can be inferred that the selected model is capable of capturing the experimentally observed loading trends and magnitudes for the entire loading regime. Although some deviations were noticed in the load-deflection response of

the specimens, these could be attributed to several factors. The higher initial stiffness of the FE model results could be traced to the likely presence of micro-cracks in the experimental specimen. These could occur through dry shrinkage of concrete and/or handling of the beams. It is also worthy to state that the accuracy of the materials parameters strongly influenced the observed response.

Notwithstanding the above, the predicted failure loads and mid-pan deflections compared well with the experimental values. As summarised in Table 5, the mean ratio of experimental to FE model results of the failure loads and deflections is 1.05 and 0.73 respectively.

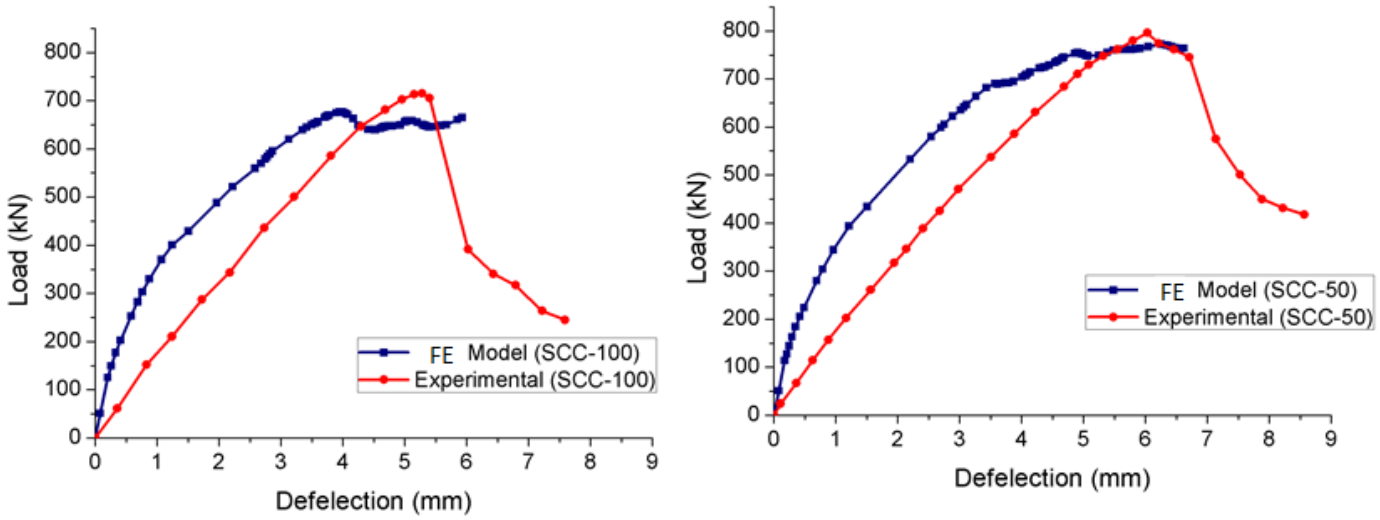

Fig. 10. FE model versus experimental load-deflection curve for the beams

4.1.2. Diagonal Cracking and Reserved Capacity

At initial loading stages, elastic stress distribution exists in all the specimen leading to flexural cracks at the lower part of the beam between loading points in the mid-span region (Figure 11). As the loading increases, the first diagonal crack developed within the shear span; the elastic stress distribution was disrupted hence the load path changed and forces flowed directly from the loaded points to the supports. This phenomenon is known as arch action in which compression struts connects the loaded points to the support and the tensile reinforcements act as ties linking the supports. The wide margin between the diagonal cracking strength and the ultimate strength could be linked to the arch action mechanism. The average ratio of the experimental to FE model

reserved capacity of the beams, which is expressed as the ratio of the diagonal cracking load to the failure/ultimate load (Pc/Pu), is 1.01 as given in Table 5.

Table 5. Experimental and FE model diagonal cracking load (Pc), ultimate load (Pu), Reserved Capacity and maximum deflection (δ) for RSCC deep beams.

Beam Code	Experimental				Experimental / FE Model			
	Pc (kN)	Pu (kN)	Reserve Capacity (Pc/Pu)	δ (mm)	Pc (kN)	Pu (kN)	Reserve Capacity (Pc/Pu)	δ (mm)
SCC 100	245	715	0.34	2.10	1.01	1.01	1.00	0.68
SCC 50	324	796	0.34	2.60	1.10	1.09	1.01	0.78
				Average	1.06	1.05	1.01	0.73

4.1.3. Failure Mode

The failures of reinforced concrete members are characterised by the occurrence and development of cracks, crushing of concrete as well as yielding of reinforcement. The crack patterns for the beams compare well with the experimental results throughout the loading regime. Figure 10 compares the cracks observe during the experiment with the cracks predicted in the simulations for SCC-50 specimen. The figure shows that at peak load, the beam failed through the diagonal crack developed within the shear span. Although there are some flexural cracks at bottom of the mid-span, it does penetrate the compression strut. Therefore, the failure of the beam is obviously a shear failure. It need to be emphasized that the concrete damaged plasticity model does not have the notion of cracks developing at the material integration point. However, it is possible to introduce the concept of an effective crack direction with the purpose of obtaining a graphical visualization of the cracking patterns in the concrete structure. The criteria adopted in this model are the assumptions that cracking initiates at points where the tensile equivalent plastic strain is greater than zero, and the maximum principal plastic strain is positive. Based on these criteria, the direction of the vector normal to the crack plane was assumed to be parallel to the direction of the maximum principal plastic strain. This direction was viewed in the visualization module of the post-processor of Abaqus CAE.

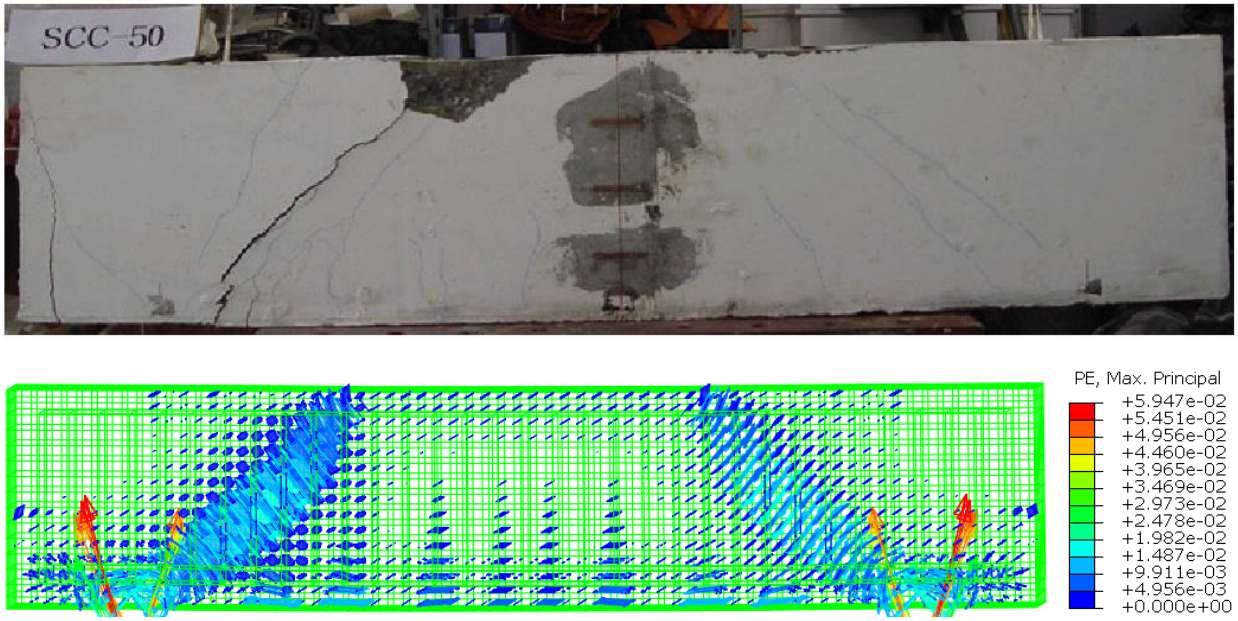

Fig. 11. Experimental and FE model crack pattern at failure for specimen SCC-50

4.2. Parametric Study

This section discussed the influence of the studied beam parameters on the diagonal cracking (Pc) and ultimate load capacity (Pu) of deep beam using the FE model. The parameters considered are concrete compressive strength (f_c), vertical web reinforcement ratio (r_v) and horizontal web reinforcement ratio (r_h).

4.2.1. Effect of Concrete Compressive Strength (f_c)

Table 6 illustrates the effect of f_c on the cracking and ultimate load for all the modelled beam specimens. The percentage increase in ultimate load due to doubling the f_c value ranges from 46.34 % to 50.39 % (average increase of 49 %). The improvements slightly reduce with increasing vertical and horizontal web reinforcement ratio. The improvement in diagonal cracking load due to doubling the fc value ranges from 39.75 % to 42.96 % (average increase of 41.1 %). The percentage increase slightly drops with increasing horizontal web reinforcement. The ratios of cracking to ultimate load range from 0.43 to 0.52 for NSCC beams while the range is 0.41 to 0.49 for HSCC beams. These show that the strength ratio decreases with increasing f_c. This is similar to the experimental result of Al-Khafaji et al. [4].

Table 6. Effect of f_c on diagonal cracking and ultimate load

	r_v %	Normal Strength (f_c = 26.0 N/mm^2)			High Strength (f_c = 52.1 N/mm^2)			% Variation due to increase in f_c	
		Pc	Pu	Pc/Pu	Pc	Pu	Pc/Pu	Pc	Pu
r_h = 0.31	0.31	223	451.3	0.49	318.8	681.4	0.47	42.96	50.99
	0.63	229	526.85	0.43	324	783.87	0.41	41.48	48.78
r_h = 0.63	0.31	239	459.26	0.52	334	686.53	0.49	39.75	49.49
	0.63	244	536.65	0.45	345	785.34	0.44	41.39	46.34

Figure 12 shows the influence of f_c on the load-deflection response of the beam specimens. From the figure, the increase in (f_c) value reduces the deflection for all the loading regime. This could be traced to the fact that increase in f_c value results in higher modulus of elasticity which then increase the flexural rigidity of the member and therefore lowers the deflection as previously observed by Al-Khafaji et al. [4].

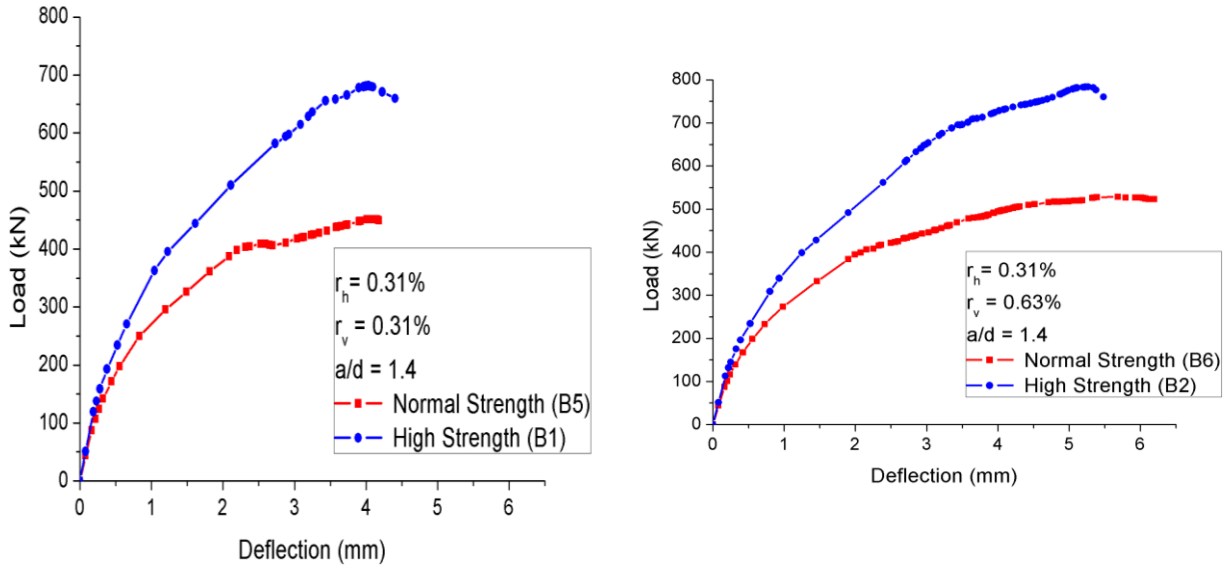

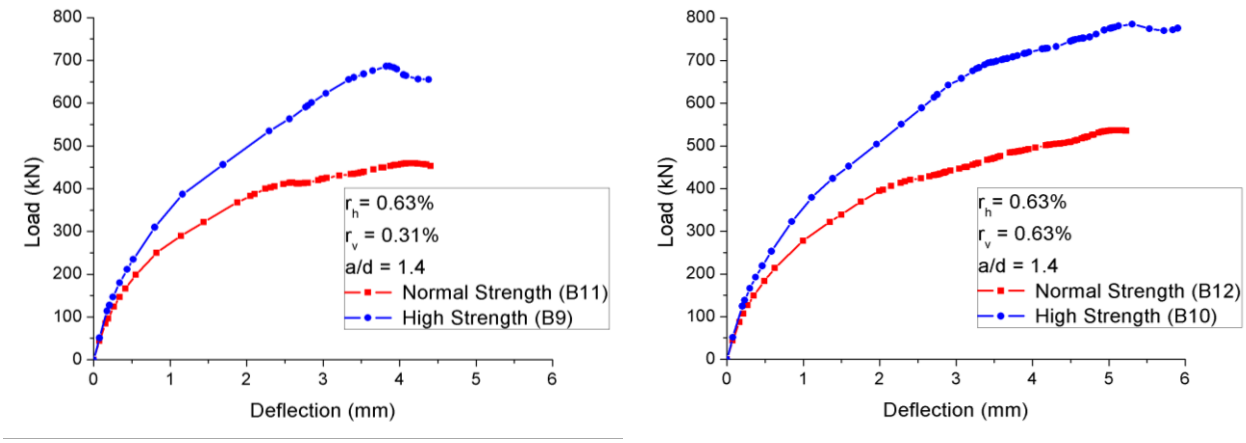

Fig. 12. Effect of f_c on load-deflection response

4.2.2. Effect of Vertical Web Reinforcement Ratio (r_v)

The effects of r_v on the cracking and the ultimate loads is shown in Table 7. Increase in r_v generally has positive influence on the cracking and the ultimate loads of the modelled beam specimens. The percentage increase in ultimate load due to doubling of r_v ranges from 14.39 to 16.85 % (average increase of 15 %). The percentage increment slightly reduces with increasing value of compressive strength (f_c). The implication is that the effect of the increase in f_c outweighs the influence of the increase in r_v. This agrees with the experimental work of Mohammadhassani et al. [24]

The percentage increment in ultimate load increases with increasing r_h for normal strength beam while the case is reversed for high strength beams. This further buttress the contribution of high strength concrete to the ultimate strength. Therefore, exceeding the minimum value of horizontal web reinforcement for high strength beams is less beneficial to the ultimate strength.

The percentage increase in the diagonal cracking load varies between 1.63 % to 3.29 % (average increase of 2.4 %). The effect of r_h on the percentage increment due to r_v depends on the compressive strength of concrete. The percentage improvement slightly drops with increasing r_h for normal strength beam while it increases significantly with increasing r_h for high strength beam. This means that higher horizontal web reinforcement benefits more in crack control for high strength beams which is contrary to the conclusion of Mohammadhassani et al. [24] that the web reinforcements do no influence the diagonal cracking load.

The ratio of cracking load to ultimate loads also decreases with increasing r_v, this implies that increasing r_v contribute more to the ultimate load than the cracking load.

Table 7. Effect of r_v on diagonal cracking and ultimate load

	r_h %	r_v%= 0.31			r_v% = 0.63			% Variation due to increase in r_v	
		P_{cr}	P_u	P_{cr}/P_u	Pcr	Pu	P_{cr}/P_u	P_{cr}	P_u
f_c= 26.0	0.31	223	451.3	0.49	229	526.85	0.43	2.69	16.74
N/mm^2	0.63	239	459.26	0.52	244	536.65	0.45	2.09	16.85
f_c= 52.1	0.31	318.8	681.4	0.47	324	783.87	0.41	1.63	15.04
N/mm^2	0.63	334	686.53	0.49	345	785.34	0.44	3.29	14.39

The plots in Figure 13 illustrate that the increase in vertical web reinforcement (r_v) does not influence the load-deflection response of the beam. Therefore, each pair of beams that only differ in r_v have convergent load-deflection response. This is due to the fact that r_v does not contribute to flexural rigidity of the beam as previously observed by Al-khafaji et al. [4].

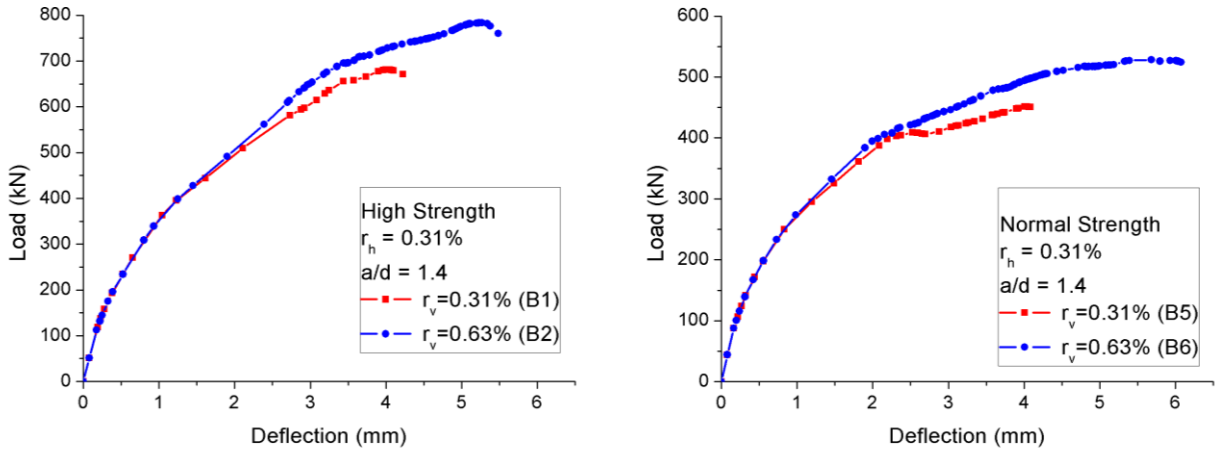

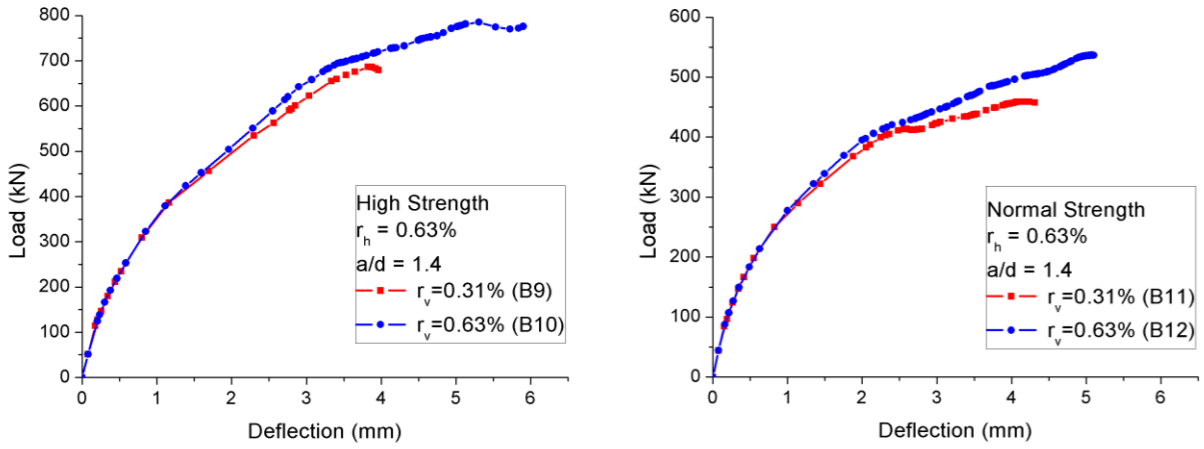

Fig. 13. Effect of r_v on load-deflection response

4.2.3. Effect of Horizontal Web Reinforcement Ratio (r_h)

The parametric effects of r_h on the cracking and the ultimate loads of the beam specimens is computed in Table 8. Unlike vertical web reinforcement (r_v), increase in r_h only contributes little or no influence to the ultimate loads of the modelled beam specimens. The percentage increase in ultimate load due to doubling of r_h ranges from 0.19 % to 1.86 % (average increase of 1.14 %). The percentage increment reduces with increasing value of compressive strength (fc). This effect is similar to that of vertical web reinforcement. This result further established the influence of f_c on the ultimate strength of deep beam.

The percentage increment in ultimate load increases with increasing r_v for normal strength beam while the case is reversed for high strength beams. This is also similar to the result of horizontal web reinforcement (r_h) although the vertical web reinforcement contributes more to the ultimate strength when compared to horizontal web reinforcement.

As seen in table 8, increase in horizontal web reinforcement ratio generally improves the diagonal cracking load of the beams. This is also contrary to the observation of Mohammadhassani [24]. The percentage increase in the diagonal cracking varies between 4.77 % to 7.17 % (average increase of 6.24 %). The percentage improvement decreases with increasing f_c for all the beam specimen. Also, the percentage improvement slightly drops with increasing r_v for normal strength beam while it increases significantly with increasing r_v for high

strength beam. This means that combination of high horizontal and vertical web reinforcement is more effective in crack control for high strength beams than normal strength beams.

Table 8. Effect of r_h on diagonal cracking and ultimate load

	r_v %	r_h %= 0.31			r_h %= 0.63			% Variation due to increase in r_h	
		P_{cr}	P_u	P_{cr}/P_u	Pcr	Pu	P_{cr}/P_u	P_{cr}	P_u
f_c= 26.0	0.31	223	451.30	0.49	239	459.26	0.52	7.17	1.76
N/mm^2	0.63	229	526.85	0.43	244	536.65	0.45	6.55	1.86
f_c= 52.1	0.31	318.8	681.4	0.47	334	686.53	0.49	4.77	0.75
N/mm^2	0.63	324	783.87	0.41	345	785.34	0.44	6.48	0.19

As seen in Figure 14, variation in horizontal web reinforcement (r_h) does not influence the load-deflection response of the studied beams. Therefore, each pair of beams that only differ in r_h have convergent load-deflection response. This is also due to the fact that r_h does not contribute to flexural rigidity of the beams.

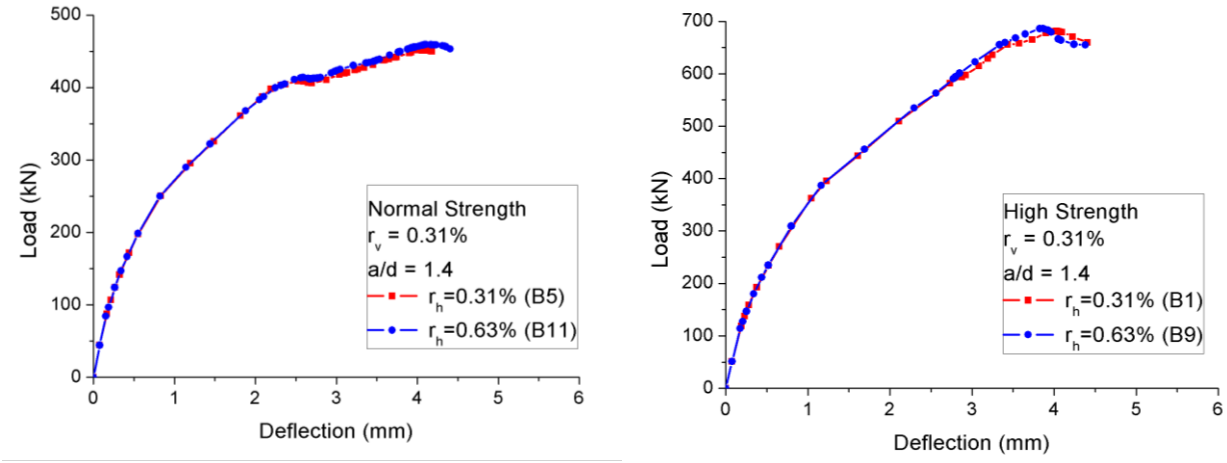

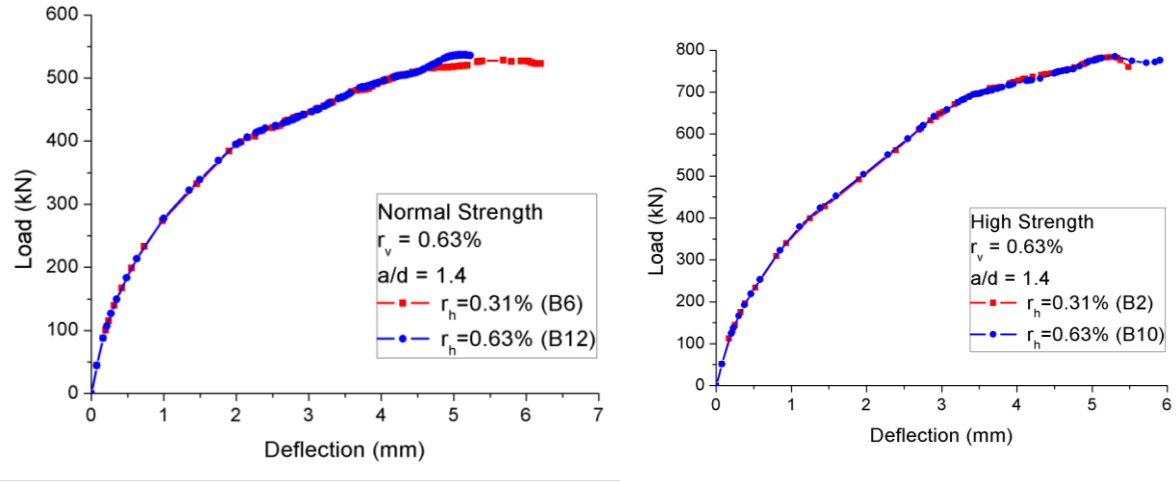

Fig. 14. Effect of r_h on load-deflection response

5. Conclusions

Finite element analysis of reinforced self-compacting concrete deep beam was conducted using Abaqus modelling tool. The model was validated against experimental results from literature and sensitivity of the model to varied dilation angle was studied. The parametric effect of varied value of concrete compressive strength, vertical web reinforcement ratio and horizontal web reinforcement ratio on the diagonal cracking and ultimate load capacity as well as load-deflection response of deep beam were also evaluated. Based on the results of this study, the followings are concluded:

(1) The FE model is capable of simulating the entire loading response of a reinforced concrete deep beam with reasonable accuracy. The mean ratio of experimental to predicted value of diagonal strength is 1.06, ultimate capacity is 1.05 and mid-span deflection is 0.73.

(2) The compressive strength of concrete has the most significant influence on the deflection, the cracking and the ultimate load of deep beam when compared with other parameters investigated. This observation conforms with the experimental study of Al-Khafaji et al. [4] and Mohammadhassani el at. [24] on self-compacting concrete deep beam.

(3) The average percentage increase in diagonal cracking and ultimate load due to doubling of concrete compressive strength is 41.1% and 49 % respectively for the studied beams.

(4) The vertical web reinforcement and the horizontal web reinforcement does not have influence on the load-deflection response of RSCC deep beam.

(5) The vertical web reinforcement ratio (r_v) of deep beam contributes more to the ultimate strength than to the diagonal cracking strength. The average percentage increase in the diagonal cracking and ultimate load due to increase in r_v from 0.31 % to 0.63 % is 2.4 % and 15 % respectively.

(6) The horizontal web reinforcement ratio does not substantially influence the ultimate strength of the RSCC deep beam although it has more influence on the diagonal cracking strength when compared with vertical web reinforcement ratio. The average increment in diagonal cracking strength is 6.24 % due to doubling of r_h ratio while it is 2.4 % due to doubling of r_v. Therefore, r_h contributes more to the diagonal cracking strength while r_v contributes more to the ultimate strength.

REFERENCES

[1] ACI 318, Building Code Requirements for Structural Concrete and Commentary, American Concrete Institute (ACI)., 2014.

[2] Eurocode 2, "Design of concrete structures - Part 1-1: General," 2004.

[3] Russo,G.,Venir,R.,and Pauletta, M., "Reinforced Concrete Deep Beams-Shear Strength Model and Design Formula.," *ACI Structural Journal,* vol. 102, no. 3, pp. 429-437, 2005.

[4] Al-Khafaji J., Al-Shaarbaf I., and Sultan W. H., "Shear Behavior of Self Compacting Concrete Deep Beams.," *Journal of Engineering and Development,* vol. 18, no. 2, pp. 36-58, 2014.

[5] Okamura H. and Ouchi M., "Self-compacting concret," *Journal of Advance Concrete Technology,* vol. 1, no. 1, pp. 1-15, 2003.

[6] EFNARC: European Federation Dedicated to Specialist Construction Chemicals and Concrete Systems, Surrey, 2002.

[7] Mutiu A. Akinpelu, Samson O. Odeyemi, Oladipupo S. Olafusi and Fatimah Z. Muhammed, "Evaluation of splitting tensile and compressive," *Journal of King Saud University – Engineering Sciences,* 2017.

[8] Choi Y. W., Lee H. K., Chu S. B., Cheong S. H. and Jung W. Y., "Shear Behavior and Performance of Deep Beams Made with Self-Compacting Concrete," *International Journal*

of Concrete Structures and Materials, vol. 6, no. 2, p. 65–78., 2012.

[9] Itterbeeck P. V., Cauberg N., Parmentier B., Ann Van Gysel A. V.and Vandewalle L., "Shear Capacity of Self-Compacting Concrete," in *Proceedings of the Fifth North American Conference on the Design and Use of Self-Consolidating Concrete*, Chicago, Illinois, 2013.

[10] Yaw L. T., Osei J. B. and Adom-Asamoah M., "On The Non-Linear Finite Element Modelling of Self-Compacting Concrete Beams," *Journal of Structural and Transportation Studies,* vol. 2, no. 2, pp. 1-18, 2017.

[11] Anjitha M. S., and Kumar K. R., "Analytical Studies on Hybrid Self Compacting Concrete Deep Beam Using Fem Software.," *International Journal of Innovative Research in Science, Engineering and Technology,* vol. 4 , no. 5, pp. 71-77, 2015.

[12] Schlaich J., Schafer K. and Jannewin M, " Toward a Consistent Design of Structural Concrete. Special Report, CEB (Comité Euro International du Béton), 77-150.," 1987.

[13] Liang Q. Q., Uy B. and Steven G. P. , "Performance-Based Optimization for Strut-Tie Modelling of Structural Concrete," *Journal of Structural Engineering,* vol. 128, no. 6, pp. 815-823, 2002.

[14] Abaqus Analysis User's Manual, Version 6.12, Volume III: Materials (2012). Dassault Systèmes Simulia Corp., Providence, RI, USA.

[15] Abaqus Theory Manual, Version 6.12 (2012). Dassault Systèmes Simulia Corp., Providence, RI, USA.

[16] Mohamed A. R., Shoukry M. S. and Saeed J. M., "Prediction of the behavior of reinforced concrete deep beams with web openings using the finite element method," *Alexandria Engineering Journal,* vol. 53, pp. 329-339, 2014.

[17] Metwally I. M., "Nonlinear analysis of concrete deep beam reinforced with gfrp bars using finite element method," *Malaysian Journal of Civil Engineering,* vol. 26, no. 2, pp. 224-250, 2014.

[18] Genikomsou A. S. and Polak M. A., "Damaged plasticity modelling of concrete in finite element analysis of reinforced concrete slabs. „" in *9th International Conference on Fracture Mechanics of Concrete and Concrete Structures University of California*, Berkeley, United State May 22- 25, 2016.

[19] Comité Euro-International du Béton, CEB-FIP-model Code , "Design code, 1990," London, Thomas Telford,, 1993.

[20] Sümer Y. and Aktas M, "Defining parameters for concrete damage plasticity model," *Challenge Journal of Structural Mechanics,* vol. 1, no. 3, p. 149–155, 2015.

[21] Demir A., Ozturk H., and Dok G., "3D Numerical Modeling of RC Deep Beam Behavior by Nonlinear Finite Element Analysis," *Disaster Science and Engineering,* vol. 2, no. 1, pp. 13-18, 2016.

[22] Michal Szczecina and Andrzej Winnicki, "Calibration of the CDP model parameters in Abaqus.," in *World Congress on Advances in structural Engineering and Mechanics (ASEM 15)*, Incheon Korea, August 25 -29.

[23] Jankowiak T. and Odygowski T., "Identification of Parameters of Concrete," *Foundation of Civil and Environmental Engineering,* no. 6, pp. 53-69, 2005.

[24] Mohammadhassani M., Jumaat M., Ashour A., Jameel M., "Failure modes and serviceability of high strength self compacting concrete deep beams," *Engineering Failure Analysis,* vol. 18, pp. 2271-2281, 2011.